Magnetic Model Refinement via a Perturbation Finite Element Method - From 1-D to 3-D

Patrick Dular, Ruth V. Sabariego, Laurent Krähenbühl

Magnetic Model Refinement via a Perturbation Finite Element Method – From 1-D to 3-D

Patrick Dular[1,2], Ruth V. Sabariego[1] and Laurent Krähenbühl[3]
[1] University of Liège, Dept. of Electrical Engineering and Computer Science, ACE, [2] FNRS, B-4000 Liège, Belgium
[3] Université de Lyon, Ampère (UMR CNRS 5005), École Centrale de Lyon, F-69134 Écully Cedex, France
E-mail: Patrick.Dular@ulg.ac.be

***Abstract*: Model refinements of magnetic circuits are performed via a subproblem finite element method based on a perturbation technique. A simplified problem considering ideal flux tubes is first solved, as either a 1-D magnetic circuit or a simplified finite element problem. Its solution is then corrected via finite element perturbation problems considering the actual flux tube geometry and the exterior regions, that allow first 2-D and then 3-D leakage fluxes. The procedure simplifies both meshing and solving processes, and quantifies the gain given by each model refinement on both local fields and global quantities.**

***Keywords*: Finite element method, magnetic circuit, model refinement, perturbation method.**

I. INTRODUCTION

The perturbation of finite element (FE) solutions provides clear advantages in repetitive analyses [1]-[2] and helps improving the solution accuracy [3]-[5]. It allows to benefit from previous computations instead of starting a new complete FE solution for any variation of geometrical or physical data. It also allows different problem-adapted meshes and computational efficiency due to the reduced size of each subproblem.

A perturbation FE method is herein developed for refining the magnetic flux distribution in magnetic circuits starting from simplified models, based on ideal flux tubes defining 1-D models, that evolve towards 2-D and 3-D accurate models. It is an extension of the method proposed in [4]-[5], applied to refinements up to 3-D models. From the so calculated field corrections, the associate corrections of global quantities proper to magnetic circuits, i.e. fluxes and magnetomotive forces (MMFs), are also evaluated to determine reluctances [6]. The method aims to build accurate reluctance networks, possibly starting from preliminary approximations [7]. The developments are performed for the magnetic vector potential FE magnetostatic formulation, paying special attention to the proper discretization of the constraints involved in each subproblem. The method is illustrated and validated on test problems.

II. MAGNETIC MODEL REFINEMENT

A. Series of coupled subproblems

Instead of solving a complete problem with all its complexity and details, it is proposed to start from a simplified problem that is then refined. The initial assumptions are thus progressively canceled via successive model refinements, i.e. with well posed subproblems.

Each subproblem is defined in its own domain, generally distinct from the complete domain. At the discrete level, this decreases the problem complexity and allows distinct meshes with suitable refinements. Many kinds of refinements can be considered, e.g. [3]-[5]. Focus is here given to refinements from 1-D to 3-D models, leading to the coupling of 1-D, 2-D and 3-D meshes.

A complete problem is thus split in a series of subproblems p of an ordered set P. Its solution $\boldsymbol{u}$ is expressed as the sum of subproblem solutions $\mathbf{u}_p$, or corrections, i.e.

$$\boldsymbol{u} = \sum_{p\in P} \boldsymbol{u}_p \,. \tag{1}$$

In general, each subproblem p is perturbed by all the other subproblems q in P, i.e. all the subproblems are coupled. This is usually obvious for $p > q$ with the defined series. For $p < q$, it is the case when a correction becomes a significant source for any of its source problems, which is inherent to large perturbation problems. It is also the case in nonlinear analyses, thus even for $p = q$. These dependencies require iterations on the set P to calculate each solution $\mathbf{u}_p$ as a series of corrections $\mathbf{u}_{p,i}$, i.e.

$$\boldsymbol{u}_p = \sum_i \boldsymbol{u}_{p,i} = \boldsymbol{u}_{p,1} + \boldsymbol{u}_{p,2} + \dots \,, \tag{2}$$

where the calculation of $\mathbf{u}_{p,i}$ in a subproblem p,i (problem p with particular constraints at iteration i) is kept on till convergence up to a desired accuracy. Each correction must account for the influence of all the previous corrections $\mathbf{u}_{p,j}$ of the other subproblems, with j the last iteration index for which a correction is known. Initial solutions $\mathbf{u}_{p,0}$ are set to zero. The global quantities linearly related to each correction, i.e. the fluxes and MMFs [6], are added to obtain their complete values. This way, they gain in accuracy for the benefit of more accurate magnetic circuit models.

B. Canonical magnetostatic problem

A canonical magnetostatic problem p is defined in a domain Ω_p, with boundary $\partial\Omega_p = \Gamma_p = \Gamma_{h,p} \cup \Gamma_{b,p}$ (possibly at infinity). Subscript p refers to the associated problem p. The equations, material relations, boundary conditions (BCs) and interface conditions (ICs) of problem p are

$$\operatorname{curl} \boldsymbol{h}_p = \boldsymbol{j}_p \,, \quad \operatorname{div} \boldsymbol{b}_p = 0 \,, \tag{3a-b}$$
$$\boldsymbol{b}_p = \mu_p \boldsymbol{h}_p + \boldsymbol{b}_{s,p} \,, \quad \boldsymbol{j}_p = \boldsymbol{j}_{s,p} \,, \tag{3c-d}$$
$$\boldsymbol{n} \times \boldsymbol{h}_p|_{\Gamma_{h,p}} = 0 \,, \quad \boldsymbol{n} \cdot \boldsymbol{b}_p|_{\Gamma_{b,p}} = 0 \,, \tag{3e-f}$$
$$[\boldsymbol{n} \times \boldsymbol{h}_p]_{\gamma_p} = \boldsymbol{j}_{su,p} \,, \quad [\boldsymbol{n} \cdot \boldsymbol{b}_p]_{\gamma_p} = \boldsymbol{b}_{su,p} \,, \tag{3g-h}$$

where $\boldsymbol{h}_p$ is the magnetic field, $\boldsymbol{b}_p$ is the magnetic flux density, $\boldsymbol{j}_p$ is the electric current density, μ_p is the

magnetic permeability and $\boldsymbol{n}$ is the unit normal exterior to Ω_p.

The fields $\boldsymbol{b}_{s,p}$ and $\boldsymbol{j}_{s,p}$ are volume sources. The source $\boldsymbol{b}_{s,p}$ is usually used for fixing a remnant induction in magnetic materials. The source $\boldsymbol{j}_{s,p}$ fixes the current density in inductors. With the perturbation method, $\boldsymbol{b}_{s,p}$ is also used for expressing changes of permeability and $\boldsymbol{j}_{s,p}$ for adding portions of inductors [5]. In magnetodynamic problems, $\boldsymbol{j}_{s,p}$ also expresses changes of conductivity [2].

The notation $[\,\cdot\,]_\gamma = \cdot|_{\gamma^+} - \cdot|_{\gamma^-}$ expresses the discontinuity of a quantity through any interface γ (with sides γ^+ and γ^-) in Ω_p (the region in between is considered to be exterior to Ω_p). The associated surface fields $\boldsymbol{j}_{su,p}$ and $\boldsymbol{b}_{su,p}$ are generally zero, defining classical ICs for the physical fields, i.e. the continuities of the tangential component of $\boldsymbol{h}_p$ and of the normal component of $\boldsymbol{b}_p$. If nonzero, they define possible surface sources that account for particular phenomena occurring in the idealized thin region between γ^+ and γ^-.

For the refinement of flux tubes, each problem p is to be constrained via the so defined surface sources from parts of the solution of other problems. This is a key element of the developed method, that can be generalized to both 2-D and 3-D problems.

III. Refinement of Flux Tubes

A. *Parallel perturbations: considering leakage flux*

In a first problem, e.g. $p=1$, the magnetic flux is forced to flow only in a subregion with perfect flux walls, i.e. a set of flux tubes $\Omega_1 = \Omega_{ft,1}$ of the complete domain Ω. A second problem, e.g. $p=2$, considers then that some flux wall portions become permeable. This allows leakage flux in the exterior region $\Omega \setminus \Omega_1$ and leads to a change of the flux distribution in Ω_1. This procedure defines a so called parallel perturbation, offering other parallel paths to the flux. A solution refinement is thus achieved.

There is a certain freedom to chose the flux wall portions to be perturbed and the sequence of such perturbations (Fig. 1). Leakage flux can be first allowed in a 2-D model [4], [5] before being extended in the third direction, i.e. in 3-D. Once flux walls become progressively permeable, the actual geometry of the inductors can be taken into account.

In problem 1, the ideal flux tubes are considered with a zero normal magnetic flux density BC on their boundaries or flux walls $\Gamma_{ft,1} = \partial\Omega_1$. The trace of the magnetic field is unknown on $\Gamma_{ft,1}$. Once determined from the solution in Ω_1, it can be used as a BC to calculate the solution in $\Omega \setminus \Omega_1$, with all the precise characteristics of this exterior region (e.g., inductors and other surrounding regions). This task is however avoided, preferring the magnetic field to be simply zero in $\Omega \setminus \Omega_1$. With that purpose, problem 1 gathers all the inductor parts of the exterior region inside the double layer defined by $\Gamma_{ft,1}^+$ and $\Gamma_{ft,1}^-$, the inner and outer sides of $\Gamma_{ft,1}$ with regard to Ω_1 (Fig. 2, *left*). This defines idealized inductors and allows the magnetic field to be zero in $\Omega \setminus \Omega_1$. Each problem $p>1$ must then correct the already obtained solutions, in particular solution 1, via particular corrections of ICs (Fig. 2, *right*). Such ICs are surface sources (or interface-type sources) fixing the possible trace discontinuities of $\boldsymbol{h}_p$ and $\boldsymbol{b}_p$ in terms of other solutions q. The forced discontinuities introduced in a problem are thus to be corrected by another one.

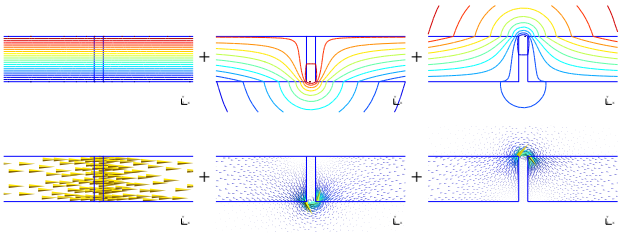

Fig. 1. Field lines (top) and magnetic flux density (bottom) of the initial problem with an ideal flux tube ($\boldsymbol{b}_1$, *left*), and its local correction below ($\boldsymbol{b}_2$, *middle*) and above the air gap ($\boldsymbol{b}_3$, *right*).

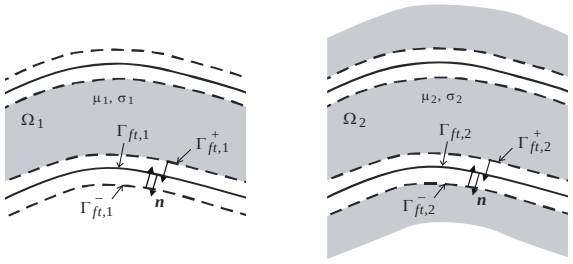

Fig. 2. Domains for the ideal (*left*) and real (*right*) flux tube problems.

The BCs of problem 1 are thus

$$\boldsymbol{n}\cdot\boldsymbol{b}_1|_{\Gamma_{ft,1}{}^+} = 0\,, \quad \boldsymbol{n}\cdot\boldsymbol{b}_1|_{\Gamma_{ft,1}{}^-} = 0\,, \qquad \text{(4a-b)}$$

$$\boldsymbol{n}\times\boldsymbol{h}_1|_{\Gamma_{ft,1}{}^+} = \boldsymbol{j}_{su,1}\,, \quad \boldsymbol{n}\times\boldsymbol{h}_1|_{\Gamma_{ft,1}{}^-} = 0\,, \qquad \text{(5a-b)}$$

which establishes the discontinuities or ICs:

$$[\boldsymbol{n}\cdot\boldsymbol{b}_1]_{\Gamma_{ft,1}} = \boldsymbol{b}_{su,1} = 0\,, \quad [\boldsymbol{n}\times\boldsymbol{h}_1]_{\Gamma_{ft,1}} = \boldsymbol{j}_{su,1}\,. \qquad \text{(6a-b)}$$

Problem 2 must correct the solution 1 via appropriate ICs (3g-h). On the one hand, one has

$$[\boldsymbol{n}\cdot\boldsymbol{b}_2]_{\Gamma_{ft,2}} = \boldsymbol{b}_{su,2} = [\boldsymbol{n}\cdot\boldsymbol{b}]_{\Gamma_{ft,2}} - \boldsymbol{b}_{su,1} = 0\,, \qquad (7)$$

due to the known continuity of $\boldsymbol{n}\cdot\boldsymbol{b}$ in the complete solution (1) and the zero value of $\boldsymbol{b}_{su,1}$ via (6a). On the other hand, one has

$$[\boldsymbol{n}\times\boldsymbol{h}_2]_{\Gamma_{ft,2}} = \boldsymbol{j}_{su,2} = [\boldsymbol{n}\times\boldsymbol{h}]_{\Gamma_{ft,2}} - \boldsymbol{j}_{su,1} = -\boldsymbol{n}\times\boldsymbol{h}_1|_{\Gamma_{ft,1}{}^+}\,, \qquad (8)$$

due to the known continuity of $\boldsymbol{n}\times\boldsymbol{h}$ in the complete solution (1) and relation (5a). Problem 2 extends then the solution out of the flux tubes and corrects it in the tubes. IC (8) can be seen as a surface source acting on both sides of $\Gamma_{ft,2}$. Note that $\Gamma_{ft,2}$ is similar to $\Gamma_{ft,1}$. They only differ at the discrete level due to their different supporting meshes.

B. *Series perturbations: connecting two flux tubes*

Prior to considering leakage flux, the series connection of two ideal flux tubes can be refined using the same kind of surface sources as in the parallel perturbations, this time as a so called series perturbation. The field distribution in each tube can be first easily constructed via geometrical considerations, i.e. no need of FE analysis (Fig. 3, *left*). In general, the flux conservation

from one tube to the other can be expressed exactly. Consequently, the junction surface now acts as an interface $\Gamma_{ft,1}$, through which the continuity of the normal magnetic flux density is satisfied ($[\boldsymbol{n}\cdot\boldsymbol{b}_1]_{\Gamma_{ft,1}}=0$) and the discontinuity of the tangential magnetic field is simply quantifiable ($[\boldsymbol{n}\times\boldsymbol{h}_1]_{\Gamma_{ft,1}}\neq 0$). The correction problem ($p=2$) to be solved is thus defined with the following ICs:

$$[\boldsymbol{n}\cdot\boldsymbol{b}_2]_{\Gamma_{ft,2}}=-[\boldsymbol{n}\cdot\boldsymbol{b}_1]_{\Gamma_{ft,1}}=0\,, \qquad (9)$$

$$[\boldsymbol{n}\times\boldsymbol{h}_2]_{\Gamma_{ft,2}}=-[\boldsymbol{n}\times\boldsymbol{h}_1]_{\Gamma_{ft,1}}\,. \qquad (10)$$

It can be limited to a certain neighborhood Ω_2 on both sides of the interface $\Gamma_{ft,2}=\Gamma_{ft,1}$ (Fig. 3, *middle*).

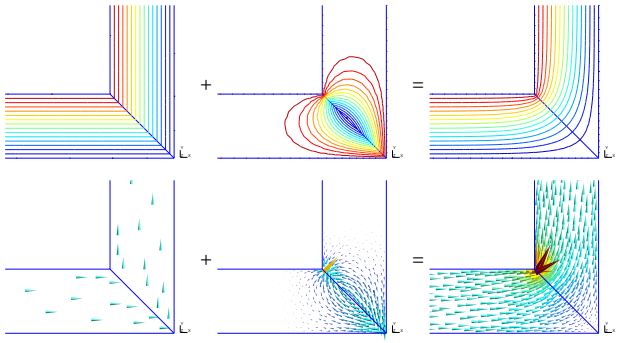

Fig. 3. Field lines (top) and magnetic flux density (bottom) of the initial problem with two ideal flux tubes in series ($\boldsymbol{b}_1$, *left*), its local correction at the junction ($\boldsymbol{b}_2$, *middle*) and the complete solution ($\boldsymbol{b}$, *right*).

IV. Finite Element Weak Formulations

A. *b-conform weak formulations*

The canonical problem p (3a-h) is defined in Ω_p with the magnetic vector potential formulation [6], expressing the magnetic flux density $\boldsymbol{b}_p$ in Ω_p as the curl of a magnetic vector potential $\boldsymbol{a}_p$. The related $\boldsymbol{a}$-formulation is obtained from the weak form of the Ampère equation (3 a), i.e. [6],

$$\begin{aligned}&(\mu_p^{-1}\,\mathrm{curl}\,\boldsymbol{a}_p,\mathrm{curl}\,\boldsymbol{a}')_{\Omega_p}-(\boldsymbol{h}_{s,p},\mathrm{curl}\,\boldsymbol{a}')_{\Omega_p}-(\boldsymbol{j}_{s,p},\boldsymbol{a}')_{\Omega_p}\\&\quad+<\boldsymbol{n}\times\boldsymbol{h}_{s,p},\boldsymbol{a}'>_{\Gamma_{h,p}}+<\boldsymbol{n}\times\boldsymbol{h}_p,\boldsymbol{a}'>_{\Gamma_{b,p}}\\&\quad+<[\boldsymbol{n}\times\boldsymbol{h}_p]_{\gamma_p},\boldsymbol{a}'>_{\gamma_p}=0\,,\quad\forall\,\boldsymbol{a}'\in F_p^{\,1}(\Omega_p)\,,\end{aligned} \qquad (11)$$

where $F_p^{\,1}(\Omega_p)$ is a gauged curl-conform function space defined on Ω_p and containing the basis functions for $\boldsymbol{a}$ as well as for the test function $\boldsymbol{a}'$ (at the discrete level, this space is defined by edge FEs); $(\cdot,\cdot)_\Omega$ and $<\cdot,\cdot>_\Gamma$ respectively denote a volume integral in Ω and a surface integral on Γ of the product of their vector field arguments. With the $\boldsymbol{b}$-conform formulation used, ICs (3 h) and (3g) are to be defined respectively in strong and weak senses (essential and natural ICs), i.e. in $F_p^{\,1}(\Omega_p)$ and in a surface integral term. The surface integral term on $\Gamma_{h,\mathrm{p}}$ accounts for natural BCs of type (3e), usually with $\boldsymbol{n}\times\boldsymbol{h}_{s,p}|_{\Gamma_{h,p}}=0$. The unknown term on the surface $\Gamma_{b,p}$ with essential BCs on $\boldsymbol{n}\cdot\boldsymbol{b}_p$ is usually omitted because it does not locally contribute to (11). It will be shown to be the key for the post-processing of a solution p, a part of which, $\boldsymbol{n}\times\boldsymbol{h}_p|_{\Gamma_{b,p}}$, is used as a source in further problems.

B. *Surface sources for leakage flux*

For the ideal flux tubes $\Omega_{ft,1}$ of problem $p=1$, BC (4a) leads to an essential BC on the primary unknown $\boldsymbol{a}_1$ that can be expressed in general (in 3-D) via the definition of a surface scalar potential u_1 [6], i.e.,

$$\boldsymbol{n}\cdot\mathrm{curl}\,\boldsymbol{a}_1\big|_{\Gamma_{ft,1}}=0\Leftrightarrow\boldsymbol{n}\times\boldsymbol{a}_1\big|_{\Gamma_{ft,1}}=\boldsymbol{n}\times\mathrm{grad}\,u_1\big|_{\Gamma_{ft,1}}\,. \qquad (12)$$

This potential is multi-valued because a net magnetic flux flows in $\Omega_{ft,1}$. Its discontinuity through cut lines, making the boundary $\Gamma_{ft,1}$ simply connected, is directly related to the net flux. In 2-D, the flux wall BC amounts to define a floating magnetic vector potential $\boldsymbol{a}_1$ (with a constant perpendicular component) on each non-connected part of $\Gamma_{ft,1}$.

Formulation $p=1$ is obtained from (11) with $\boldsymbol{b}_{s,1}=0$, $\boldsymbol{j}_{s,1}=0$, $\boldsymbol{n}\times\boldsymbol{h}_{s,1}|_{\Gamma_{h,1}}=0$, $\Gamma_{ft,1}\subset\Gamma_{b,1}$ and $\gamma_1=\varnothing$. The surface integral term $<\boldsymbol{n}\times\boldsymbol{h}_1,\boldsymbol{a}'>_{\Gamma_{ft,1}}$ differs from zero only for the test function $\boldsymbol{a}'=\mathrm{grad}\,u'$ (from (12)), the value of which is then the MMF F_1 associated with a flux tube (this can be demonstrated from the general procedure developed in [6]). It is zero for all the other local test functions (at the discrete level, for any edge not belonging to $\Gamma_{ft,1}$). This way, the magnetic circuit relation can be expressed for each flux tube $\Omega_{ft,1}$, to relate fluxes and MMFs.

The correction formulation $p=2$ is then obtained from (11) with $\boldsymbol{b}_{s,2}=0$, $\boldsymbol{n}\times\boldsymbol{h}_{s,2}|_{\Gamma_{h,2}}=0$ and $\gamma_2=\Gamma_{ft,2}$. The volume source current density $\boldsymbol{j}_{s,2}$ is now defined in the inductor portions added to the studied domain Ω_2, in place of the firstly idealized inductors. IC (7) is strongly expressed via the essential tangential continuity of the vector potential $\boldsymbol{a}_2$ through $\Gamma_{ft,2}$. IC (8) can rather only act in a weak sense via the surface integral term related to $\gamma_2=\Gamma_{ft,2}$ in (11). Indeed, the involved surface source $\boldsymbol{n}\times\boldsymbol{h}_1$ is not known in a strong sense on $\Gamma_{ft,2}$, but rather in a weak sense. One has, with (8) and (11) for $p=1$,

$$\begin{aligned}&<[\boldsymbol{n}\times\boldsymbol{h}_2]_{\Gamma_{ft,2}},\boldsymbol{a}'>_{\Gamma_{ft,2}}=<-\boldsymbol{n}\times\boldsymbol{h}_1,\boldsymbol{a}'>_{\Gamma_{ft,2}^{\,+}}\\&=<-\boldsymbol{n}\times\boldsymbol{h}_1,\boldsymbol{a}'>_{\Gamma_{ft,1}^{\,+}}=(\mu_1^{-1}\,\mathrm{curl}\,\boldsymbol{a}_1,\mathrm{curl}\,\boldsymbol{a}')_{\Omega_{ft,1}=\Omega_{ft,2}}\,.\end{aligned} \qquad (13)$$

This way, the surface integral source term on $\gamma_2=\Gamma_{ft,2}$ in (11) is calculated from a volume integral coming from the previous problem 1. Its consideration via a volume integral, limited at the discrete level to one single layer of FEs touching the boundary, is the natural way to average it as a weak quantity. Any other kind of evaluation would not be consistent with the FE formulation used.

At the discrete level, the source quantity $\boldsymbol{a}_1$ in (13), initially given in mesh 1, has to be projected in mesh 2 in a domain $\Omega_{s,2}$ limited to the layer of FEs touching $\Gamma_{ft,2}$. This can be done via a Galerkin projection method [8] of its curl limited to $\Omega_{s,2}$, i.e.

$$\begin{aligned}(\mathrm{curl}\,\boldsymbol{a}_{1,2\text{-}proj},\mathrm{curl}\,\boldsymbol{a}')_{\Omega_{s,2}}&=(\mathrm{curl}\,\boldsymbol{a}_1,\mathrm{curl}\,\boldsymbol{a}')_{\Omega_{s,2}}\,,\\&\forall\,\boldsymbol{a}'\in F_2^{\,1}(\Omega_{s,2})\,,\end{aligned} \qquad (14)$$

where $F_2^{\,1}(\Omega_{s,2})$ is a gauged curl-conform function space for the 2-projected source $\boldsymbol{a}_{1,2\text{-}proj}$ (the projection of $\boldsymbol{a}_1$

on mesh 2) and the test function $\boldsymbol{a}'$. Directly projecting $\boldsymbol{a}_1$ (not its curl) would result in numerical inaccuracies when evaluating its curl.

The test function $\boldsymbol{a}'$ in (13) is associated only with the edges of $\Gamma_{ft,2}$; the support of the function curl $\boldsymbol{a}'$ is indeed limited to this layer. This reduced support decreases the computational effort of the projection process.

C. *Surface sources for a series connection of flux tubes*

The local FE problem to be solved in the neighborhood of a junction interface $\Gamma_{ft,2} = \Gamma_{ft,1}$ of two flux tubes is still expressed by (11). IC (9) leads to the tangential continuity of the vector potential $\boldsymbol{a}_2$ through $\Gamma_{ft,2}$. IC (10) is weakly expressed via the surface source integral term

$$<[\boldsymbol{n}\times\boldsymbol{h}_2]_{\Gamma_{ft,2}},\boldsymbol{a}'>_{\Gamma_{ft,2}} = <-[\boldsymbol{n}\times\boldsymbol{h}_1]_{\Gamma_{ft,1}},\boldsymbol{a}'>_{\Gamma_{ft,2}}, \quad (15)$$

which is simply calculated from the known distribution of $\boldsymbol{h}_1$ on both sides of $\Gamma_{ft,1}$.

V. Application

Two problems are considered to test and illustrate the refinement method from 1-D to 3-D models.

A stranded inductor is first studied (Fig. 4). Its cross section in the XY plane initially defines an initial 2-D model, with the solution shown in Fig. 4 (*left*). This 2-D solution is considered to be invariant in the Z direction up to a certain distance (z = 100 mm). Beyond this distance, the field is chosen to be zero, which results in a particular IC to be further corrected. This solution then serves as an IC constraint (8) for a 3-D perturbation model considering the inductor end winding.

A part of the correction is shown in a plane crossing the end winding, where its significance in the direct vicinity of this end region is pointed out (Fig. 4, *right*). Another part is shown along a line centered with the inductor and following its main (Z) direction (Fig. 5).

The current density distribution considered for the 2-D model is implicitly the one shown in Fig. 6, *left*. Once this distribution has been used in 2-D, the 3-D perturbation model only needs its complementary part defined in the end windings (Fig. 6, *right*).

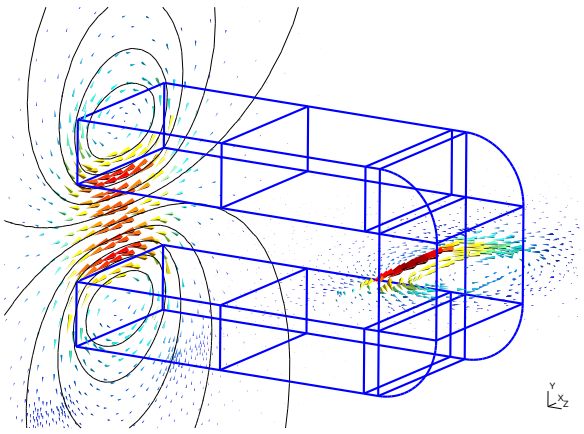

Fig. 4. Magnetic flux density generated by a stranded inductor (half geometry): solution of the 2-D model in the XY plane (z = 0) (vector field and field lines, *left*) and a part of the 3-D correction in a particular plane crossing the end winding (*right*).

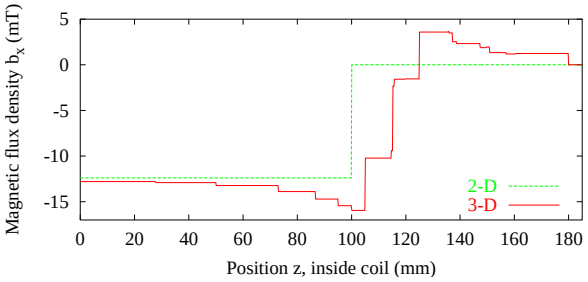

Fig. 5. Magnetic flux density along the main (Z) direction of the inductor (from its center): solution of the 2-D model (implicitly extended as a constant up to z = 100 mm) and 3-D solution after correction in the vicinity of the end winding.

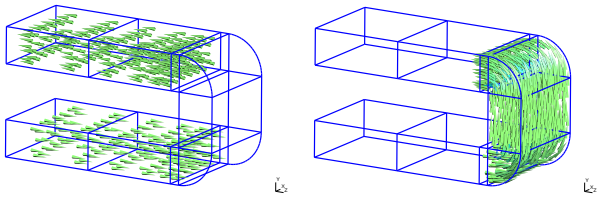

Fig. 6. Source current density in the inductor: its implicit distribution for the 2-D model (*left*) and its complementary part in the end winding for the 3-D perturbation model (*right*).

An electromagnet is then studied (Fig. 7). It consists of a U-shape core surrounded by a stranded inductor and separated from an I-shape core via two air gaps. For both core, the width and depth are 20 mm and 100 mm respectively. Their relative permeability is $\mu_{r,U\text{-}core} = \mu_{r,I\text{-}core} = 500$. Each gap is 3 mm. Other values of the permeability and the air gap will be considered as well for parameterized analyses.

A 2-D solution is first calculated (Fig. 8). It can be either obtained directly or from a sequence of correction problems starting from a 1-D model progressively refined in 2-D with consideration of 2-D leakage fluxes [4], [5]. This solution serves then as a source for a perturbation problem allowing leakage flux in 3-D, in the same way it has been done with only the inductor. Significant corrections near the end winding and the air gaps are shown (Figs. 9 and 10). The 3-D problem calculates the actual flux distribution in the vicinity of the inductor end winding and in the vicinity of the cores, with its own adapted mesh. It also corrects the flux density in the cores and the air gaps.

Each correction properly modifies the inductor flux linkage. This is shown for air gaps of 1 mm and 3 mm in Figs. 11 and 12 respectively. The 1-D model simply considers ideal flux tubes of constant sections. It is then followed by a 2-D model considering ideal flux tubes with their actual geometry (corners are thus accurately taken into account). Then leakage fluxes in and out of the flux tubes are considered in 2-D as well, before extension in the third dimension (3-D). In general, each additional leakage flux correction significantly influences the inductor flux linkage. The 3-D correction is lower for low reluctances of the magnetic circuit (i.e. for high permeability and small air gap).

The relative corrections obtained for model refinements from 1-D to 2-D and from 2-D to 3-D are given in Figs. 13 and 14 respectively, for different air gaps (0 mm, 1 mm and 3 mm) in function of the permeability of the magnetic cores. Neglecting 2-D

leakage fluxes obviously amounts to large errors (about 50%) in magnetic circuits with higher reluctances (e.g. larger air gaps and/or lower permeability). Neglecting 3-D leakage fluxes amounts to an error up to 25% for the considered geometry. The error will be higher with flatter magnetic circuits.

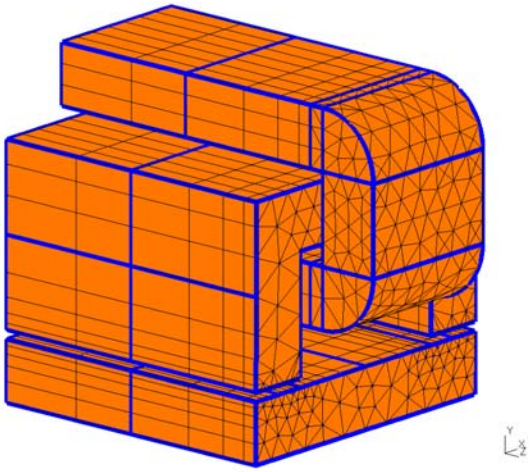

Fig. 7. 3-D model of the electromagnet (*left*); its 2-D cross section and solution (magnetic flux density and field lines) (*right*).

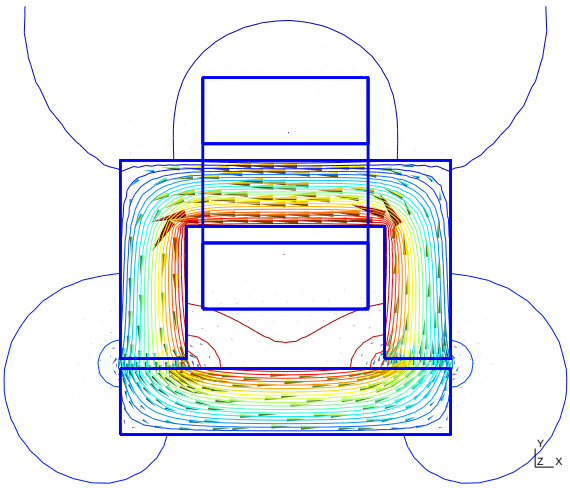

Fig. 8. 3-D model of the electromagnet (*left*); its 2-D cross section and solution (magnetic flux density and field lines) (*right*).

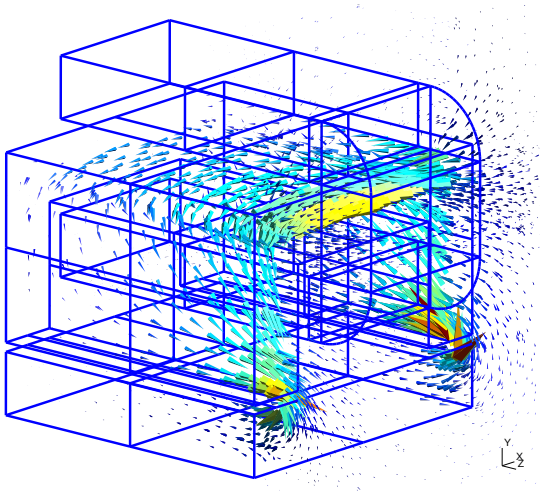

Fig. 9. Magnetic flux density: solution of the 3-D correction in particular planes near the end winding and the air gaps.

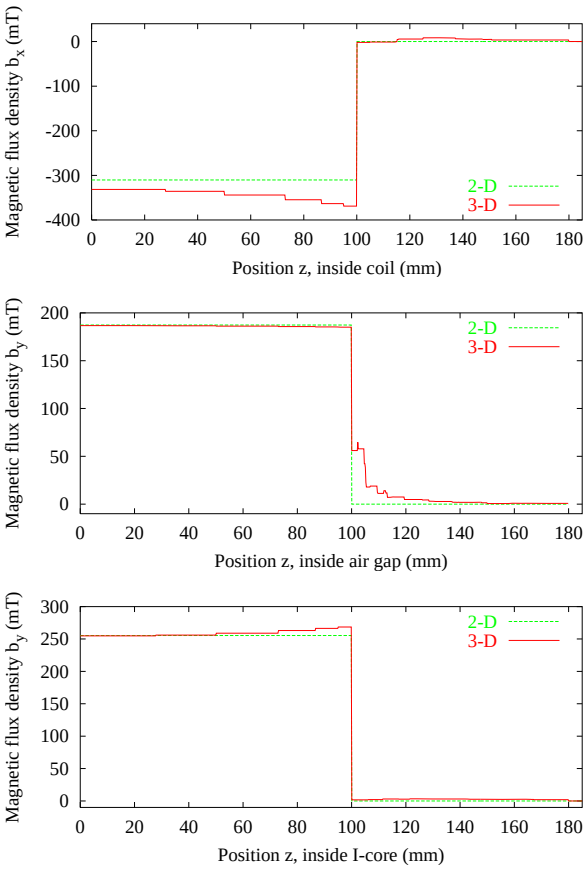

Fig. 10. Magnetic flux density along Z direction in the 3-D system: solution of the 2-D model (implicitly extended as a constant up to z = 100 mm) and 3-D solution after corrections in the vicinity of the end winding (*top*), the air gap (*middle*) and the I-core (*bottom*).

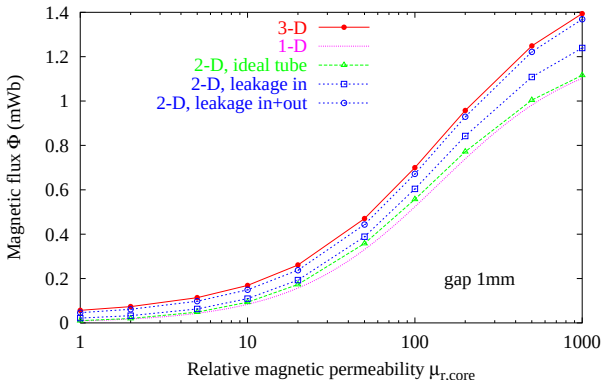

Fig. 11. Inductor flux linkage versus the core magnetic permeability (air gap thickness of 1 mm) updated after each model refinement.

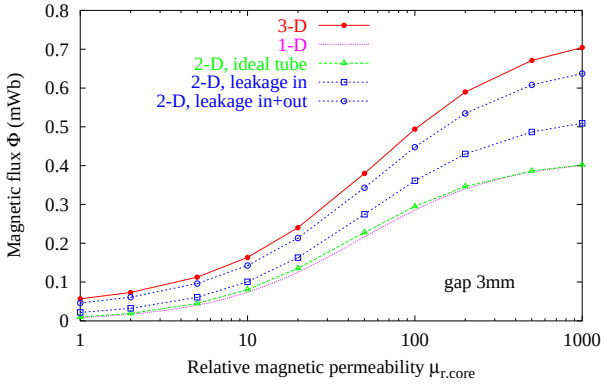

Fig. 12. Inductor flux linkage versus the core magnetic permeability (air gap thickness of 3 mm) updated after each model refinement.

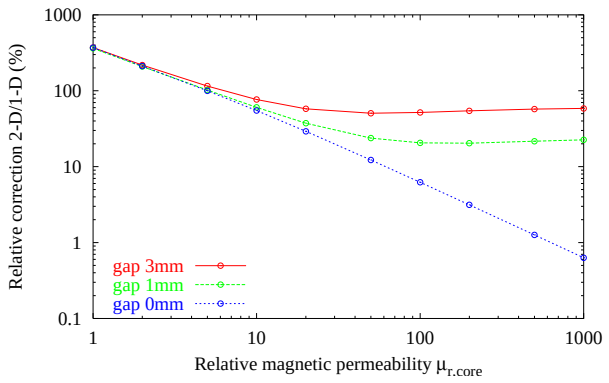

Fig. 13. Relative correction from 1-D to 2-D models versus the core magnetic permeability for different air gap thicknesses.

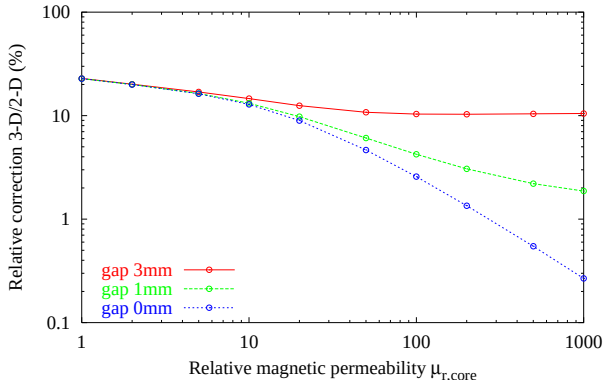

Fig. 14. Relative correction from 2-D to 3-D models versus the core magnetic permeability for different air gap thicknesses.

For each series of subproblems, the convergence of the solution depends on the extension of the subdomains. The more extended the subdomains are, the faster the convergence is. At the limit, if the successive subdomains progressively cover the complete domain, no iterations are needed. This paper focuses on the practical aspects of the method, mainly the surface sources that can appear in perturbation FE analyses from 1-D to 3-D. A detailed study of the convergence is out of the scope of this preliminary paper.

VI. Conclusions

The developed perturbation FE method allows to split magnetic circuit analyses into subproblems of lower complexity with regard to meshing operations and computational aspects. A natural progression from simple to more elaborate models, from 1-D to 3-D geometries, is thus possible, while quantifying the gain given by each model refinement and justifying its utility. Approximate problems with ideal flux tubes are accurately corrected when accounting for leakage fluxes via surface sources of perturbations. The constraints involved in the subproblems have been carefully defined in the resulting FE formulations, respecting their inherent strong and weak nature. As a result, an efficient and accurate computation of local fields and global quantities, i.e. flux, MMF, reluctance, is obtained. The method is naturally adapted to parameterized analyses on geometrical and material data.

Further work is in progress for defining additional types of subproblems, e.g. to apply successive perturbations accounting for nonlinear and eddy current models. An adaptation of the domain of each subproblem has to be also studied, together with its effect on the convergence of the complete solution.

Acknowledgment

This work was partly supported by the Fund for Scientific Research Belgium (F.R.S.-FNRS), the Belgian Science Policy (IAP P6/21) and the Walloon Region.

References

[1] Z. Badics, Y. Matsumoto, K. Aoki, F. Nakayasu, M. Uesaka and K. Miya, “An effective 3-D finite element scheme for computing electromagnetic field distorsions due to defects in eddy-current nondestructive evaluation,” *IEEE Trans. Magn.*, Vol. 33, No. 2, pp. 1012-1020, 1997.

[2] P. Dular and R. V. Sabariego, “A perturbation method for computing field distortions due to conductive regions with h-conform magnetodynamic finite element formulations,” *IEEE Trans. Magn.*, Vol. 43, No. 4, pp. 1293-1296, 2007.

[3] P. Dular, R. V. Sabariego, J. Gyselinck and L. Krähenbühl, “Sub-domain finite element method for efficiently considering strong skin and proximity effects,” *COMPEL*, Vol. 26, No. 4, pp. 974-985, 2007.

[4] P. Dular, R. V. Sabariego, M. V. Ferreira da Luz, P. Kuo-Peng and L. Krähenbühl, “Perturbation Finite Element Method for Magnetic Model Refinement of Air Gaps and Leakage Fluxes,” *CEFC 2008, to be published in IEEE Trans. Magn.*, Vol. 45, 2009.

[5] P. Dular, R.V. Sabariego, M.V. Ferreira da Luz, P. Kuo-Peng and L. Krähenbühl, “Perturbation finite-element method for magnetic circuits,” *IET Science, Measurement & Technology*, Vol. 2, No. 6, 2008.

[6] P. Dular, J. Gyselinck, T. Henneron and F. Piriou, “Dual finite element formulations for lumped reluctances coupling,” *IEEE Trans. Magn.*, Vol. 41, No. 5, pp. 1396-1399, 2005.

[7] C. Chillet and J.Y. Voyant, “Design-oriented analytical study of a linear electromagnetic actuator by means of a reluctance network,” *IEEE Trans. Magn.*, Vol. 37, No. 4, pp. 3004-3011, 2001.

[8] C. Geuzaine, B. Meys, F. Henrotte, P. Dular and W. Legros, “A Galerkin projection method for mixed finite elements,” *IEEE Trans. Magn.*, Vol. 35, No. 3, pp. 1438-1441, 1999.